Title
Noninvasive Two-Photon Microscopy Imaging of Mouse Retina and Retinal Pigment Epithelium

Authors
Palczewska, Grazyna
Kern, Timothy S
Palczewski, Krzysztof

Publication Date
2019

DOI
10.1007/978-1-4939-8669-9_21

Peer reviewed

HHS Public Access

Author manuscript

Methods Mol Biol. Author manuscript; available in PMC 2020 January 30.

Published in final edited form as:

Methods Mol Biol. 2019 ; 1834: 333–343. doi:10.1007/978-1-4939-8669-9_21.

Noninvasive two-photon microscopy imaging of mouse retina and retinal pigmented epithelium

Grazyna Palczewska[1], **Timothy S. Kern**[2], **Krzysztof Palczewski**[2]

[1]Polgenix Inc., 11000 Cedar Ave., Cleveland, Ohio 44106

[2]Department of Pharmacology, Case Western Reserve University School of Medicine, 10900 Euclid Avenue, Cleveland, Ohio 44106

Abstract

Two-photon excitation microscopy is suited for imaging deep into the retina due to its use of infra-red (IR) wavelengths to excite endogenous fluorophores such as vitamin A-derived retinoids present in this tissue. Furthermore, two-photon excitation occurs only around a small focal volume, and scattered IR photons cannot excite retinal chromophores. These characteristics contribute to the subcellular resolution and low noise of images obtained deep within retinal layers. Here we describe how to customize a two-photon microscope for noninvasive imaging of the retina and retinal pigmented epithelium (RPE) in the mouse eye, along with detailed instructions for mouse handling and retinal imaging. Examples of mouse retinal two-photon microscopy data are also provided.

Keywords

Two-photon microscopy; mouse eye; retina; RPE; vitamin A

1. Introduction

Two-photon microscopy (TPM), which derives its imaging contrast from the two-photon excited fluorescence (TPEF) of fluorophores present in a tissue, is a powerful method for monitoring biochemical processes that sustain our vision, evaluating retinal pathologies, and assessing the impact of therapeutics on retinal preservation. For TPEF to occur, a fluorophore must absorb two photons of impinging light within the time frame of the light cycle, on the order of 0.5 fs for near infrared light (IR), where fs stands for femtoseconds (10^{-15} of a second). The sum of the energy of these two photons needs to approximate the energy of a single photon required for one-photon excited fluorescence. Thus, two IR photons can excite a molecule with an absorption maximum in the visible light range. However, the two-photon absorption cross section ($\boldsymbol{\sigma_2}$) is in the range of $\sigma_2 \approx 10^{-52}$ cm^4s per photon [1], as compared with a single-photon absorption cross section ($\boldsymbol{\sigma_1}$) with a $\sigma_1 \approx 10^{-17}$ cm^2 [2]. Thus, to achieve appreciable TPEF, photons impinging on the fluorophore need to be compressed in both time and space. Development of mode-locked lasers delivering 100 fs pulses at an 80 MHz pulse repetition frequency yielded high transient

concentrations of photons in time, and resulted in a successful demonstration of TPEF imaging of live cultured pig kidney cells [3]. In that study, a high numerical aperture (NA) was used to condense photons in space. Such an arrangement allowed the demonstration of quadratic dependence of TPEF on excitation light intensity, which was implied by the theory of two-photon absorption developed Maria Goppert-Mayer [4]. Thus, light scattered by tissue does not contribute to TPEF, and two-photon excitation occurs only around a focal volume. Moreover, a pinhole, employed in confocal microscopes to reject fluorescence coming from outside the focal volume, is not needed in the detection path, and all the fluorescence photons can be collected by a detector.

TPM has contributed to significant advances in understanding biochemical processes in the eye. Retinosomes, organelles that store retinyl esters in the RPE, were discovered by applying TPEF to image mouse RPE *in vivo* and *ex vivo* [5,6]. TPEF microscopy of intact mouse eyes with different excitation wavelengths revealed two types of vitamin A derived retinoids: 1) condensation products which accumulate with age in the RPE and over-accumulate in an animal model of human Stargardt disease, namely $Abca4^{-/-}Rdh8^{-/-}$ mice and 2) retinyl esters that participate in the visual cycle. Imaging revealed the subcellular distribution of these fluorophores and their changes in aging mice [7,8]. Improvement in focusing the excitation beam, accomplished by integration of sensor-less adaptive optics (AO) with TPEF microscopy, resulted in subcellular images of the RPE and ganglion cells in living mice, based on endogenous fluorophores [9]. Cua *et al.* applied coherence-gated sensor-less AO to visualize TPEF from retinal capillaries in living mice subcutaneously injected with fluorescein [10]. Furthermore, TPEF with traditional, wavefront sensor-based AO was applied to image ganglion cells labeled with both GFP and G-CaMP3 [11], (Note 1). Quantification of early changes in photoreceptor structures after exposure to bright light and the impact of pharmacological treatment also was accomplished with a high quantum yield, actively cooled HYD detector [12].

2. Materials

2.1 Animals.

Mice can be obtained from the Jackson Laboratory (Bar Harbor, ME, USA) or other institutions.

2.2 Equipment

1. Vision-S with built-in dispersion pre-compensation (Coherent, Santa Clara, CA, USA)
2. Laser power meter, PM100D (Thorlabs, Newton, NJ, USA)
3. Laser power meter sensor, S120C (Thorlabs, Newton NJ, USA)
4. Low magnification sectioning microscope
5. Mouse holder, custom made (Fig. 1a)

[1]When using TPM in combination with additional measurements of retinal function, remember that visual pigments can be activated by the IR light typically employed in TPM [16].

6. Objective for *in vivo* imaging: Leica HCX FL PLAN 10x/0.25 (Leica Microsystems Inc., Buffalo Grove, IL, USA). This objective has a working distance of 17.6 mm
7. Objective for *ex vivo* imaging: Leica HCX APO L 20x/1.00 W (Leica Microsystems Inc., Buffalo Grove, IL, USA). This is a water immersion objective with 2 mm working distance.
8. Deformable mirror with 140 actuators, continuous surface, gold coating and 5.5 μm stroke, (Boston Micromachines Corp., Cambridge, MA, USA)

2.2 Supplies

1. Genteal lubricant eye gel (Alcon Laboratories, Fort Worth, TX, USA)
2. Renu fresh multi-purpose contact lens solution (Bausch & Lomb, Rochester, NY, USA)
3. Refresh Plus, lubricant eye drops (Allergan Inc., Irvine, CA, USA)
4. Super Glue Gel (Super Glue Corporation, Ontario, CA, USA)
5. Phosphate–buffered saline (1xPBS) (ThermoFisher, Waltham, MA, USA)
6. Eye spears (DeRoyal, Powell, TN, USA)
7. Kimwipes (Kimberly-Clark Inc., Roswell, GA, USA)
8. Puritan double pointed tip cotton swabs (Harmony Business Supplies, Garden Grove, CA, USA)
9. Petri dishes, 35 mm diameter, 10 mm tall (ThermoFisher Scientific, Waltham, MA, USA)
10. Spring scissors with curved tip and 10 mm long cutting edge (FST, Foster City, CA, USA)
11. Plastic tip tweezers, (Excelta Corporation, Buellton, CA, USA)
12. Micro-M lens, 3.2 mm diameter, 0 diopter contact lens (Cantor and Nissel, Northamptonshire, UK)
13. Micro-M lens, 3.2 mm diameter, −50 diopter contact lens (Cantor and Nissel, Northamptonshire, UK)

3. Methods

3.1 Mice

All animal procedures, including anesthesia and euthanasia, should be approved by an Institutional Animal Care and Use Committee and conform to both the recommendations of the American Veterinary Medical Association and the Association for Research in Vision and Ophthalmology.

3.2 Microscope configuration

1. Room illumination. Low-laser power, high signal-to-noise ratio images can be achieved if there are no sources of parasitic light in the microscope room. Therefore, it is critical to obtain images with all lights turned off, and to isolate the space between the mouse eye and the detector with the use of black enclosures, preferably black plastic or anodized aluminum.

2. Light source. A pulsing laser is essential for obtaining the TPEF images without tissue alteration. A laser that delivers 75 fs pulses at an 80 MHz pulse repetition rate and is equipped with dispersion compensation and a tuning range from 690 nm to 900 nm (Note 2) is sufficient [9].

3. Light path. Non-invasive TPEF imaging of mouse retina can be achieved with a microscope equipped with a dichroic mirror that efficiently separates light backscattered by the optical system and eye structures from the fluorescence signal emitted by retinal fluorophores (Note 3) (Fig. 1). Power of the laser beam is regulated by the use of an electro-optic modulator (EOM). After the EOM, the laser beam is routed through a sensor-less adaptive optics system and then to scanners. Two sets of scanners, X and Y, span the rectangular area of the sample, typically with scanning speeds at 400 to 1000 lines per second, that result in an image acquisition rate of less than 1.5 s/frame. The TPEF signal is typically collected in a format of 512 by 512 to 1024 by 1024 pixels per image. Laser light is coupled into the mouse eye either with an objective with sufficient focal depth and working distance to reach the retina, or with a custom-designed periscope that directs the collimated laser beam (about 2.4 mm in diameter) onto the mouse eye [13]. Imaging is done in the EPI configuration such that two-photon excited fluorescence is captured by the same objective. The detector, preferably a highly sensitive hybrid detector (HYD) with active cooling, should be located as close to the objective as possible to efficiently collect two-photon excited fluorescence without de-scanning.

3.3 Adaptive optics

An increase in the TPEF signal can be achieved without increasing laser power by incorporating adaptive optics (AO) to improve the focus of the excitation beam.

1. AO design approach. Excitation is the most critical factor in TPEF because fluorescent photons are generated only around the focal volume, and are collected without a pinhole and de-scanning by a detector located close to the objective. As introduction of adaptive optics in the fluorescent light path would adversely decrease the TPEF signal, an AO system for two-photon microscopy

[2]In a typical microscope setup using 75 fs laser pulses, TPEF images obtained with optimally adjusted dispersion pre-compensation can be 5 times brighter than those obtained without dispersion pre-compensation but with the same average laser power.
[3]A microscope equipped with an upright stand can be used for both *ex vivo* and *in vivo* studies with commercially-available or custom objectives, or with a periscope. A microscope equipped with an inverted stand can be used for *ex vivo* studies. *In vivo* studies with an inverted microscope stand would require either a periscope objective or a more elaborate mouse holder to ensure stabilization of the mouse head with its eye facing down.

needs only to correct the excitation beam. AO design without a wavefront sensor is appropriate for mouse imaging.

2. AO system construction. The AO system consists of a beam expander, a beam relay, a deformable mirror (DM) and folding mirrors. The beam expander magnifies the beam just after the EOM, so that it slightly overfills the DM, whereas the beam relay, located along the light path after the DM, de-magnifies the laser beam back to its size at the entry to the AO system. Folding mirrors route the laser beam onto the DM and out to the scanners, and ensure a minimal footprint for the system [9].

3. Optimization of the surface shape of the DM. The DM is modulated based on the image quality feedback, with the use of a set of orthogonal polynomials, referred as Zernike modes, which are often used to describe ophthalmic aberrations [14]. The DM surface optimization algorithm can be integrated with the microscope imaging workstation and image collecting software. It takes less than 4 min to attain an optimal surface of the DM.

3.4 Objectives

1. Imaging the retina in live mice with a commercially-available objective. The objective needs to have sufficiently long focal depth and maximum NA. Because the mouse eye optical system (including cornea and lens) focuses the light on the retina, it is necessary to optically flatten the mouse eye when using such an objective. This can be achieved with a mouse contact lens with a flat front surface, (−50 diopter lens in Materials section). Image quality of the RPE obtained with such a lens is good in the center portion of the eye, but less so for areas outside of the central portion. Moreover, the NA of this objective is 0.25 as compared to 0.42 for the mouse eye [15], and this NA limits TPEF efficiency.

2. Custom objective for imaging the retina in a live mouse. Such an objective can be assembled using commercially-available lenses with a long focal depth, ~ 20 mm, and NA larger than 0.43. However, even with a high NA objective, a contact lens with a flat front face is still needed, so retinal images obtained outside the center portion of the eye will not have the highest quality.

3. Retinosomes in RPE cells and the condensation products can be visualized using either of the two objectives just described (Fig. 2a).

3. Periscope for imaging the retina in a live mouse. A custom optical device, called a periscope, which changes the direction of the light beam from vertical to horizontal and provides a collimated beam ~ 2.4 mm in diameter to overfill a mouse eye pupil is a more complex system [13]. The overall design of such a periscope depends on the design of the optical paths of each microscope, namely: 1) the geometry of the beam and location of the rear aperture of the regular microscope objective, and 2) the position of the pivot point conjugate with the scanners outside the microscope body. The periscope is equipped with a translation stage that changes the location of one of its lenses (and consequently changes the location of the focal point in the retina) to account for differences in

the dimensions of the mouse eye, and to allow focusing on different layers of the retina. With such a periscope, different areas of a mouse eye can be investigated by simply: 1) rotating the mouse stage around the vertical axis such that the center of rotation aligns with the pupil of the mouse eye, 2) rotating the mouse eye around the horizontal axis, and 3) adjusting the Z and X positions with the microscope stage manipulators. Only a thin, 0 diopter contact lens is needed to maintain cornea hydration during imaging with a periscope. Moreover, images obtained from different areas of the mouse retina are of comparable high quality (Fig. 2b).

3.5 Imaging *ex vivo*

Visualization of individual retinal cells including the RPE, photoreceptor outer and inner segments, and ganglion cells can be achieved in intact eyes both *in vivo* and *ex vivo* (Note 4). In *ex vivo* studies, a water immersion objective with a working distance of at least 2 mm and a NA =1.0 provides the greatest detail and permits 3D reconstruction of the arrangement of retinal cells (Fig. 3). By following the procedures outlined below, individual retinal rod photoreceptors can be resolved in *ex vivo* mouse eyes with laser light penetrating through the sclera.

The procedure below is for an upright microscope and imaging through the sclera.

1. After anesthesia and euthanasia, enucleate the eye using spring scissors with a curved tip; don’t pull on the eye as this will stretch the retina and cause distortions.
2. Place the eye in a 35 mm diameter petri dish with the sclera facing up (Figure 1b).
3. Attach the eye to the petri dish with small drops of gel super glue.
4. Fill the petri dish with 1x PBS.
5. Observe the eye with a low magnification sectioning microscope. Use eye spears pre-soaked in 1x PBS to remove any air bubbles and impurities on the tissue.
6. Place the petri dish with the eye on the TPM stage, submerge the objective face in PBS, turn off all lights, and start the TPM acquisition mode (Notes 5, 6 and 7). Observe the monitor screen while slowly moving the stage along the z-axis towards the globe. The sclera will be the first tissue visible.

[4]Albino mice can be imaged both through the sclera and through the pupil. However, pigmented mice can be imaged only through the pupil.
[5]Bi-directional scans, slower scanning speeds, and/or higher pixel counts can result in tissue damage. Thus, a unidirectional scan, 400 lines per second, and a 512×512 pixels image format covering a retinal area of about 0.5 × 0.5 mm is a good starting point for obtaining images without altering the eye tissue.
[6]If using a tunable laser, select a wavelength that is about twice the wavelength of maximal one-photon absorption for the fluorophore of interest. For wild type mice, 750 nm provides a good starting point.
[7]Because laser power can vary and optical parameters of the microscope system can change with temperature, use a laser power meter equipped with a sensor appropriate for the laser tuning range and power levels to calibrate the laser power and EOM settings at least 45 min after turning on the microscope and switching on the acquisition mode.

3.6 Imaging *in vivo*

Preparation of the mouse for imaging *in vivo* is the same whether using a periscope or the two objectives described above.

1. Using pharmaceuticals recommended by the Institutional Animal Care and Use Committee, dilate the pupils of the mouse eyes and then anesthetize the mouse.
2. Cover the mouse eye with Genteal lubricant eye gel. Wipe off excess gel with eye spears pre-soaked in 1x PBS, and then trim eyelashes.
3. Using tweezers with plastic tips, place a contact lens on the mouse eye. Don't smear Genteal gel on the front surface of the contact lens. If that happens, rinse the lens in Renu fresh multi-purpose contact lens solution and place it on a Kimwipe. While securing the lens with plastic tweezers, gently wipe the outside and inside surfaces of the lens with a Puritan double pointed tip cotton swab until the lens is completely dry and free of smudges. Re-apply the lens as described above.
4. Position the mouse on a warming stage and align the light beam between the objective and the pupil of the mouse eye. Use a visible light source for this step.
5. Turn off all lights, start the TPM acquisition mode (Notes 5, 6 and 7), and observe the monitor screen while slowly changing the distance between the mouse eye and objective. When using a regular objective, the cornea should be the first visible tissue [9].

Acknowledgements

We thank Dr. Leslie T. Webster, Jr., and members of the Palczewski laboratory for valuable comments regarding this manuscript. K.P. is Chief Scientific Officer at Polgenix. K.P. is an inventor of the U.S. patent no. 7,706,863 and U.S. patent no. 8,346,345, whose values may be affected by this publication. This research was supported in part by grants from the National Institutes of Health (NIH) (EY027283, EYU01 EY025451 and EY R24024864).

REFERENCES

1. Zipfel WR, Williams RM, Christie R, Nikitin AY et al. (2003) Live tissue intrinsic emission microscopy using multiphoton-excited native fluorescence and second harmonic generation. Proc Natl Acad Sci U S A 100:7075–7080. [PubMed: 12756303]
2. Tsina E, Chen C, Koutalos Y, Ala-Laurila P et al. (2004) Physiological and microfluorometric studies of reduction and clearance of retinal in bleached rod photoreceptors. J Gen Physiol 124:429–443. [PubMed: 15452202]
3. Denk W, Strickler JH, Webb WW (1990) Two-photon laser scanning fluorescence microscopy. Science 248:73–76. [PubMed: 2321027]
4. Pawlicki M, Collins HA, Denning RG, Anderson HL (2009) Two-photon absorption and the design of two-photon dyes. Angew Chem Int Ed Engl 48:3244–3266. [PubMed: 19370705]
5. Imanishi Y, Gerke V, Palczewski K (2004) Retinosomes: new insights into intracellular managing of hydrophobic substances in lipid bodies. J Cell Biol 166:447–453. [PubMed: 15314061]
6. Imanishi Y, Batten ML, Piston DW, Baehr W et al. (2004) Noninvasive two-photon imaging reveals retinyl ester storage structures in the eye. J Cell Biol 164:373–383. [PubMed: 14745001]
7. Palczewska G, Maeda T, Imanishi Y, Sun W et al. (2010) Noninvasive multiphoton fluorescence microscopy resolves retinol and retinal condensation products in mouse eyes. Nat Med 16:1444–1449. [PubMed: 21076393]

8. Kiser PD, Palczewski K (2016) Retinoids and Retinal Diseases. Annu Rev Vis Sci 2:197–234. [PubMed: 27917399]
9. Palczewska G, Dong Z, Golczak M, Hunter JJ et al. (2014) Noninvasive two-photon microscopy imaging of mouse retina and retinal pigment epithelium through the pupil of the eye. Nat Med 20:785–789. [PubMed: 24952647]
10. Cua M, Wahl DJ, Zhao Y, Lee S et al. (2016) Coherence-Gated Sensorless Adaptive Optics Multiphoton Retinal Imaging. Sci Rep 6:32223. [PubMed: 27599635]
11. Sharma R, Yin L, Geng Y, Merigan WH et al. (2013) In vivo two-photon imaging of the mouse retina. Biomed Opt Express 4:1285–1293. [PubMed: 24009992]
12. Maeda A, Palczewska G, Golczak M, Kohno H et al. (2014) Two-photon microscopy reveals early rod photoreceptor cell damage in light-exposed mutant mice. Proc Natl Acad Sci U S A 111:E1428–1437. [PubMed: 24706832]
13. Stremplewski P, Komar K, Palczewski K, Wojtkowski M et al. (2015) Periscope for noninvasive two-photon imaging of murine retina in vivo. Biomed Opt Express 6:3352–3361. [PubMed: 26417507]
14. Thibos LN, Applegate RA, Schwiegerling JT, Webb R et al. (2002) Standards for reporting the optical aberrations of eyes. J Refract Surg 18:S652–660. [PubMed: 12361175]
15. Zwick H, Edsall P, Stuck BE, Wood E et al. (2008) Laser induced photoreceptor damage and recovery in the high numerical aperture eye of the garter snake. Vision Res 48:486–493. [PubMed: 18252238]
16. Palczewska G, Vinberg F, Stremplewski P, Bircher MP et al. (2014) Human infrared vision is triggered by two-photon chromophore isomerization. Proc Natl Acad Sci U S A 111:E5445–5454. [PubMed: 25453064]
17. Palczewska G, Maeda A, Golczak M, Arai E et al. (2016) Receptor MER Tyrosine Kinase Proto-oncogene (MERTK) Is Not Required for Transfer of Bis-retinoids to the Retinal Pigmented Epithelium. J Biol Chem 291:26937–26949. [PubMed: 27875314]

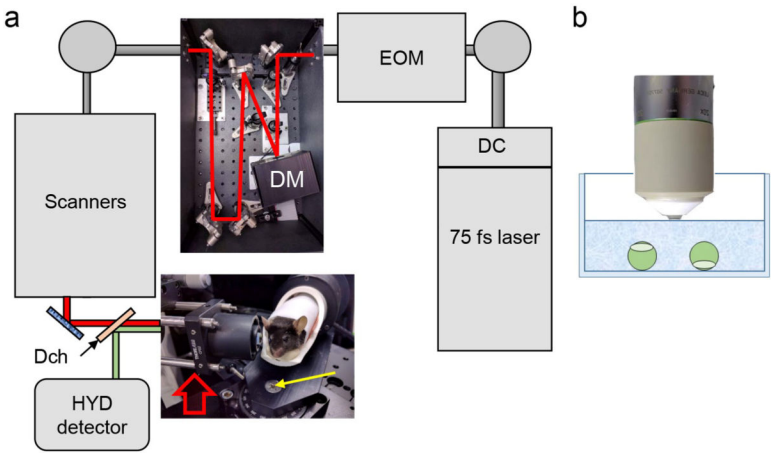

Figure 1:

System for noninvasive imaging of the retina and RPE in the mouse eye. (a) Customized microscope design. Light from a tunable laser (Vision-S; Coherent, Santa Clara, CA) is modulated with a dispersion pre-compensation unit (DC). An electro-optic modulator (EOM) is used to adjust laser power delivered to the sample. The laser light path through an adaptive optics system which includes a deformable mirror (DM) is outlined in red. Vertical and horizontal scanners route the laser beam in a rectangular pattern over the retina and RPE. A custom periscope objective [13], indicated with a red arrow, directs the laser beam into the mouse eye. An anesthetized mouse is placed on a warming stage, which can rotate around the vertical axis, wherein the center of rotation is aligned with the mouse eye and is indicated with a yellow arrow. Fluorescence (in green) is collected in a non-descanned manner. In this EPI configuration, fluorescent light emanating from the eye is collected by the same lens, and after reflecting off a dichroic mirror (Dch) is directed to an HYD detector. (b) For imaging intact eyes *ex vivo*, enucleated eyes are submerged in 1xPBS, and imaged through the pupil (left) or through the sclera (right).

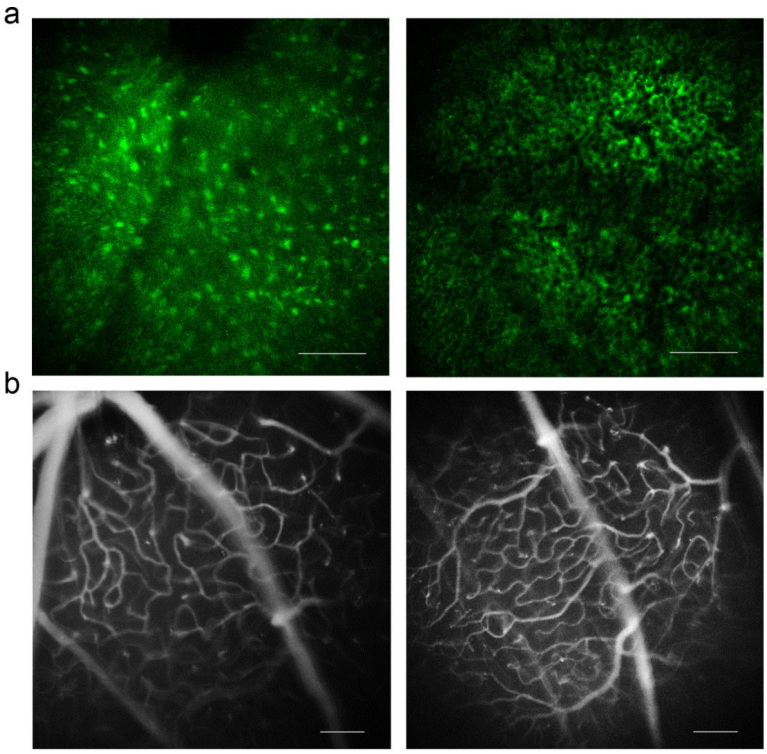

Figure 2:

TPM imaging of the retina and RPE in mouse models of retinal pathologies *in vivo*. (a) TPM imaging based on endogenous fluorophores. Left, brightly fluorescent granules of retinal condensation products are visible in the retina and RPE of 3.5-month old *Mertk*$^{-/-}$*Abca4*$^{-/-}$*Rdh8*$^{-/-}$ mice, with defective phagocytosis and retinoid cycle pathways [17]. Right, retinosomes outline the contours of RPE cells in 1-year old albino *Rpe65*$^{-/-}$ mice, a mouse model of human Leber congenital amaurosis. Both images were obtained with 800 nm laser light. (b) Visualization of retinal capillaries *in vivo*, in 1-year-old C57BL/6J-*Tyr*$^{C-2J}$ mice, after tail vain injection with a fluorescein – BSA solution. This approach can be used to evaluate leakage from retinal capillaries in mice with induced diabetes. Left and right images are from different sections of the retina in the same eye. Images were obtained with 820 nm laser light.

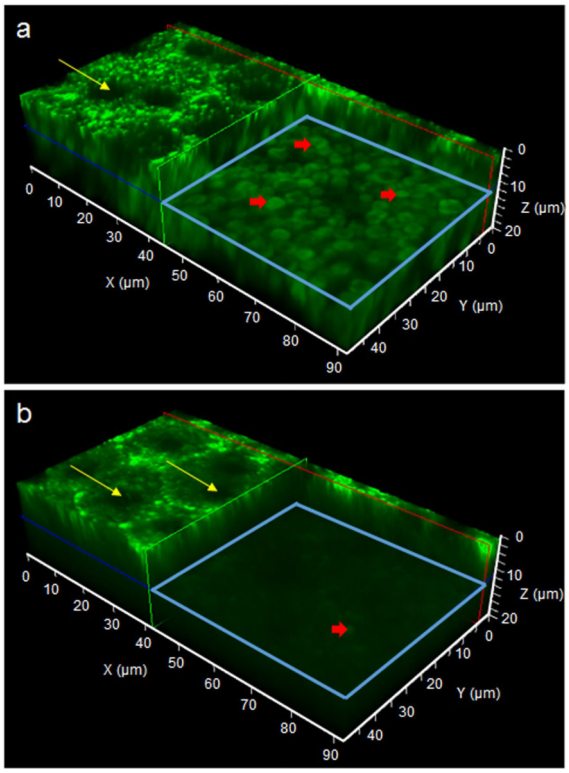

Figure 3:

Ex vivo TPM imaging of the retina after induction of photoreceptor damage in intact eyes of 1-month old albino *Abca4*$^{-/-}$*Rdh8*$^{-/-}$ mice. Reconstructed volumes obtained from a series of z-stack images obtained with 730 nm excitation light are shown in both (a) and (b). The RPE is at z=0, and the section outlined in blue is 10 μm under the RPE (towards the ganglion cell layer). Red arrows indicate enlarged photoreceptors [16], yellow arrows designate RPE nuclei. (a) Retinal 3D volume from a mouse treated with DMSO before induction of photoreceptor damage. (b) Retinal 3D volume from a mouse treated with an investigative pharmaceutical before induction of photoreceptor damage. Large quantities of enlarged photoreceptors present in mice treated with DMSO indicate severe damage to the retina.